Inorganic Chemistry

Article

pubs.acs.org/IC

Uranyl Carboxyphosphonates Derived from Hydrothermal in Situ Ligand Reaction: Syntheses, Structures, and Computational Investigations

Dai Wu,[†,∥] Xiaojing Bai,[§,‡,∥] Hong-Rui Tian,[†] Weiting Yang,*[,†] Zewen Li,[§] Qing Huang,[‡] Shiyu Du,*[,‡] and Zhong-Ming Sun*[,†]

[†]State Key Laboratory of Rare Earth Resource Utilization, Changchun Institute of Applied Chemistry, Chinese Academy of Sciences, 5625 Renmin Street, Changchun, Jilin 130022, China

[§]School of Chemistry and Materials Science, Heilongjiang University, Harbin, Heilongjiang 150080, China

[‡]Division of Functional Materials and Nanodevices, Ningbo Institute of Materials Technology and Engineering, Chinese Academy of Sciences, Ningbo, Zhejiang 315201, China

Supporting Information

ABSTRACT: Two uranyl carboxyphosphonates $(H_2dipy)[(UO_2)_3(H_2O)_2(H_2DPTP)_2]\cdot 2H_2O$ (**DPTP-U1**) and $(H_2bbi)[(UO_2)_4(H_2O)_2(HDPTP)_2]$ (**DPTP-U2**) [H_6DPTP = 2,5-diphosphonoterephthalic acid, dipy = 4,4′-bipyridine, bbi = 1,1′-(1,4-butanediyl)bis(imidazole)] were synthesized under hydrothermal conditions. The carboxyphosphonate ligand was formed through the in situ oxidation of (2,5-dimethyl-1,4-phenylene)diphosphonic acid mediated by UO_2^{2+}. Single-crystal X-ray diffraction analyses reveal that **DPTP-U1** possesses uranyl carboxyphosphonate layers that are separated by protonated dipy cations. Whereas **DPTP-U2** is in a three-dimensional framework structure with channels filled by protonated bbi cations. The computational investigations give an insight into the nature of bonding interactions between uranium(VI) and carboxyphosphonate ligand. The spectroscopic properties were also studied.

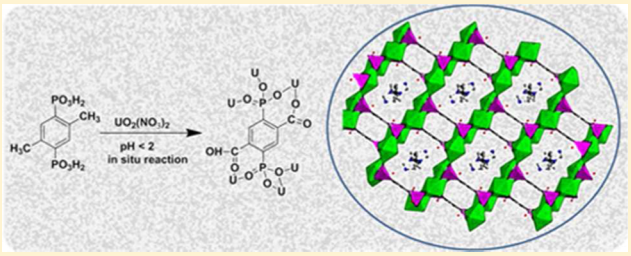

INTRODUCTION

Hydrothermal or solvothermal in situ ligand reaction involves a process wherein the organic material undergoes various reactions, such as oxidation, reduction, and displacement to form a new ligand with modified functional groups. The generated ligand is then observed in crystalline coordination polymeric products. The in situ ligand reaction plays an important role in the fields of both synthetic organic chemistry and inorganic crystal engineering.[1−3] This approach is becoming increasingly popular for its advantages of discovery of new organic reactions, elucidation of reaction mechanisms, environmental friendliness, simplified synthesis, slow ligand formation conducive for single-crystal growth, and preparation of new coordination polymers, especially those that are not accessible by direct reaction from the metal centers and organic linkers. So far, most of reported in situ ligand reactions have been explored in the presence of transition metal centers.[4−11] Recently, Cahill and co-workers have utilized such strategy to expand the actinide chemistry, and several uranium(VI) hybrid materials have been obtained.[12−15] For example, a uranyl complex of 4-(hydroxy-methyl)benzoic acid was formed via the in situ hydrolysis of 4-(bromomethyl)benzoic acid.[12] A 1,3-dipolar cycloaddition of 4-azidobenzoic acid and propiolic acid in the presence of UO_2^{2+} cation generated a uranyl triazolate.[13] Five uranyl oxalates were synthesized via the in situ oxidation of N-heterocycle organic species.[14,15] In our recent work, the in situ oxalate formation was observed during the syntheses of uranyl phosphinates.[16] These interesting studies show the potential of in situ ligand reaction in preparation of new uranium-bearing coordination complexes and arouse our interest in further exploring other ligand reactions to acquire novel uranium hybrid materials.

1,4-phenylenediphosphonic acid (H_4PDP), which possesses two PO_3 groups with strong affinity for binding metal centers, has been widely investigated for construction of coordination polymers that refer to most transition metals, lanthanides, and actinides.[17−19] However, its derivative, (2,5-dimethyl-1,4-phenylene)diphosphonic acid (H_4DMPDP), has been rarely used for isolation of coordination hybrids.[20] On the one hand, considering the rigid backbone and the phosphonate functions of the two ligands, DMPDP should be able to form similar coordination polymer structures with those constructed by PDP. On the other hand, the steric and electronic effects from the two methyl moieties can alter the coordination fashion of DMPDP, thereby resulting in different structures relative to the ones obtained by PDP. Moreover, the two methyl groups have the potential to be in situ oxidized to carboxyl functions, which

Received: June 4, 2015
Published: August 19, 2015

DOI: 10.1021/acs.inorgchem.5b01266
Inorg. Chem. 2015, 54, 8617−8624

Table 1. Crystallographic Data and Structure Refinement Parameters for Synthesized Uranyl Compounds and DPTP Ligand

compound	DPTP-U1	DPTP-U2	DPTP
empirical formula	$C_{26}H_{18}N_2O_{30}P_4U_3$	$C_{13}H_{11}N_2O_{15}P_2U_2$	$C_8H_8O_{10}P_2$
F_w	1676.39	973.24	326.08
crystal system	triclinic	triclinic	monoclinic
space group	$P\bar{1}$	$P\bar{1}$	$C2/c$
a, Å	9.6088(8)	9.7561(13)	20.743(7)
b, Å	9.7439(8)	10.2852(14)	7.692(3)
c, Å	11.0648(9)	11.0465(14)	16.960(9)
α, deg	81.842(2)	95.127(3)	90
β, deg	85.131(2)	95.109(2)	124.476(5)
γ, deg	87.5750(10)	105.974(2)	90
V, Å^3	1021.30(15)	1053.9(2)	2230.7(16)
Z	1	2	4
$F(000)$	764	874	664
ρ_{calcd} (Mg/m^3)	2.726	3.067	0.971
μ (Mo Kα)/ mm^{-1}	12.128	15.581	0.223
R_1/wR_2 ($I > 2\sigma(I)$)[a]	0.0344/0.0705	0.0509/0.12	0.0404/0.1101
R_1/wR_2 (all data)	0.0455/0.0754	0.0603/0.1236	0.0564/0.1156

[a] $R_1 = \sum(\Delta F/\sum(F_0))$; $wR_2 = (\sum[w(F_0^2 - F_c^2)])/\sum[w(F_0^2)^2]^{1/2}$, $w = 1/\sigma^2(F_0^2)$

also feature classical O-donor sites for ligating metal atoms. As a result, unexpected coordination hybrid structures could be formed during this in situ synthesis. Thus, in this work, we explored in situ oxidation of DMPDP as a means of generating uranyl (UO_2^{2+}) coordination polymers based on the following considerations: (1) The in situ oxidation of methyl group to carboxyl has been known to occur on the N-heterocycle organic species under acidic conditions,[21] while investigations on the phenyl ring are less reported. As far as we know, most uranyl phosphonates were obtained under low pH,[22−27] which facilitates the oxidation of methyl group. (2) Nitrate from the metal salts and the protons in the solution including those added for adjusting pH can act as the oxidant.[28,21b] (3) In addition to the phosphonate groups, the in situ generated carboxylate moieties can also bind uranyl centers to form intriguing uranyl hybrid coordination polymers. We herein report two novel uranyl carboxyphosphonates $(H_2dipy)[(UO_2)_3(H_2O)_2(H_2DPTP)_2]\cdot 2H_2O$ (**DPTP-U1**) and $(H_2bbi)[(UO_2)_4(H_2O)_2(HDPTP)_2]$ (**DPTP-U2**; H_6DPTP = 2,5-diphosphonoterephthalic acid, dipy = 4,4′-bipyridine, bbi = 1,1′-(1,4-butanediyl)bis(imidazole)) that are derived from in situ ligand reaction under hydrothermal condition. Their syntheses, structures, and spectroscopic properties are described. Furthermore, computational investigations are performed to elucidate the nature of interactions between U(VI) and the carboxyphosphonate ligand.

EXPERIMENTAL SECTION

Caution! *Standard procedures for handling radioactive material should be followed, although the uranyl compounds used in the lab contained depleted uranium.*

Materials, Syntheses, and Characterization. $UO_2(NO_3)_2\cdot 6H_2O$ (Aladdin Reagent, 99.5%), 4,4′-bipyridine (Aladdin Reagent, 98%) and 1,1′-(1,4-butanediyl)bis(imidazole) (Sinopharm Chemical Reagent, 99%) were purchased commercially and used without further purification. (2,5-dimethyl-1,4-phenylene)diphosphonic acid was synthesized according to a documented literature.[20] Powder X-ray diffraction (XRD) data were collected on a D8 Focus (Bruker) diffractometer at 40 kV and 30 mA with monochromated Cu Kα radiation (λ = 1.5405 Å) with a scan speed of 5 deg/min and a step size of 0.02° in 2θ. Elemental analyses of C, H, and N were conducted on a Perkin-Elmer 2400 elemental analyzer. Infrared spectra were collected from single crystals using a Nicolet 6700 FT-IR spectrometer with a diamond ATR objective. Solid-state UV−visible absorption measurement was performed using a Hitachi U-4100 spectrophotometer. The photoluminescence (PL) excitation and emission spectra were recorded with a Hitachi F-7000 luminescence spectrometer equipped with a xenon lamp of 450 W as an excitation light source. The photomultiplier tube voltage was 400 V, the scan speed was 1200 nm min^{-1}, and both the excitation and the emission slit widths were 5.0 nm.

*Synthesis of **DPTP-U1**.* A mixture of $UO_2(NO_3)_2\cdot 6H_2O$ (50 mg, 0.1 mmol), (2,5-dimethyl-1,4-phenylene)diphosphonic acid (28 mg, 0.11 mmol), dipy (10 mg, 0.064 mmol), HNO_3 (65%, 50 μL), and deionized water (1.0 mL) (pH = 1.82) was loaded into a 20 mL Teflon-lined stainless steel autoclave. The autoclave was sealed and heated at 180 °C for 3 d and then cooled to room temperature. Minor yellow blocklike product of **DPTP-U1** suitable for X-ray studies was isolated along with colorless block crystal of DPTP ligand,[28] which was confirmed by single-crystal and powder X-ray diffraction analyses (Table 1 and Figure S1). Pure powder phase of **DPTP-U1** could, however, be obtained by direct reaction of uranyl nitrate, DPTP ligand, and dipy under similar conditions. The phase purity was confirmed by the powder XRD analyses, which are shown in Figure S2. Anal. Calcd (wt %) for $C_{26}H_{18}N_2O_{30}P_4U$: C, 26.02; H, 1.51; N, 2.33. Found: C, 26.10; H, 1.57; N, 2.39.

*Synthesis of **DPTP-U2**.* A mixture of $UO_2(NO_3)_2\cdot 6H_2O$ (50 mg, 0.1 mmol), (2,5-dimethyl-1,4-phenylene)diphosphonic acid (28 mg, 0.11 mmol), bbi (10 mg, 0.053 mmol), HNO_3 (65%, 100 μL), and deionized water (1.0 mL) (pH = 1.68) was loaded into a 20 mL Teflon-lined stainless steel autoclave. The autoclave was sealed and heated at 180 °C for 3 d and then cooled to room temperature. Yellow blocklike crystals of pure **DPTP-U2** were isolated after being washed with deionized water and allowed to air-dry at room temperature. This compound could also be synthesized using DPTP as the ligand instead of DMPDP under similar conditions, which led to pure **DPTP-U2** as yellow powder. Anal. Calcd (wt %) for $C_{13}H_{11}N_2O_{15}P_2U_2$: C, 16.04; H, 1.14; N, 2.88. Found: C, 16.24; H,1.08; N, 2.75. Powder XRD pattern of the as-synthesized material confirms the phase purity as shown in Figure S3.

X-ray Crystal Structure Determination. Suitable single crystals for the two compounds and DPTP ligand were selected for single-crystal X-ray diffraction analyses. Crystallographic data were collected at 296 K on a Bruker Apex II CCD diffractometer with graphite monochromated Mo Kα radiation (λ = 0.710 73 Å). The structures were solved by direct methods and refined on F^2 by full-matrix least-squares using SHELXTL.[29] Non-hydrogen atoms were refined with anisotropic displacement parameters during the final cycles. All

DOI: 10.1021/acs.inorgchem.5b01266
Inorg. Chem. 2015, 54, 8617−8624

hydrogen atoms were placed by geometrical considerations and were added to the structure factor calculation. A summary of the crystallographic data for the two uranyl compounds and DTPT ligand are listed in Table 1. Selected bond distances and angles are given in Table S1.

Computational Methods. The models for **DPTP-U1** and **DPTP-U2** are constructed according to the corresponding experimental crystal structures. Our first-principles density functional theory[30] calculations are performed with the CASTEP codes,[31] which use a plane wave basis set for the valence electrons and norm-conserving pseudopotential for the core electron. The generalized gradient approximation (GGA)[32] of Perdew–Breke–Ernzerh (PBE)[33] functional is adopted for the exchange and correlation energy.[34] The number of plane waves is determined by a cutoff energy of E_c = 350 eV. The valence electron configurations for all atoms are chosen to be conventional, that is, H-$1s^1$, C-$2s^2 2p^2$, N-$2s^2 2p^3$, O-$2s^2 2p^4$, P-$3s^2 3p^3$, and U-$5f^3 6s^2 6p^6 6d^1 7s^2$. Total energy changes were finally reduced to less than 1×10^{-6} eV/atom, and Hellman–Feynman forces acting on atoms were converged less than 0.05 eV/Å.

RESULT AND DISCUSSION

Syntheses. Interest in syntheses of uranyl organic hybrid materials is motivated by their broad range of structural topologies and promising physicochemical properties. One effective way to expand their chemistry is using new organic ligands with strong affinity for uranium centers, such as phosphonates and carboxylates. Additionally, in situ ligand reaction is of particular interest for formation of novel uranyl organic compounds with modified ligands. In this work, (2,5-dimethyl-1,4-phenylene)diphosphonic acid (H_4DMPDP) was in situ oxidized to 2,5-diphosphonoterephthalic acid (H_6DPTP) in the presence of UO_2^{2+} under hydrothermal conditions (Scheme 1) and yielded two new uranyl carboxyphosphonate compounds, $(H_2dipy)[(UO_2)_3(H_2O)_2(H_2DPTP)_2]\cdot 2H_2O$ (**DPTP-U1**) and $(H_2bbi)[(UO_2)_4(H_2O)_2(HDPTP)_2]$ (**DPTP-U2**). However, direct assembly of uranyl nitrate and the DPTP ligand in the presence of directing agents only led to products in crystalline powder form. This demonstrates that the slow release of the ligand in situ promotes the formation of unique products suitable for single-crystal structure determination. Similar phenomenon was previously found by Albrecht-Schmitt and co-workers in preparation of uranyl carboxyphosphonates, in which the slow hydrolysis of triethylphosphonoacetate was the key step for the crystallization, and directly adding phosphonoacetate to the reactions only led to powders.[35] It is noted that in both syntheses, nitric acid must be added, which not only keeps the strong acidic condition but also may serve as the oxidant. It is well-known that alkyl chain in aromatic compound can be oxidized to carboxylic group using nitric acid.[28] For example, Tong et al. recently reported nitric acid could in situ oxidize substituted methyl group on the pyridine ring into carboxyl.[21a,b] Therefore, it is reasonable to expect a similar role may be played by nitric acid in the oxidation of DMPDP into DPTP. To elucidate this point, control experiments were performed first under unmodified pH without adding nitric acid (pH = 2.6) and second replacing $UO_2(NO_3)_2\cdot 6H_2O$ by $UO_2(OAc)_2\cdot 2H_2O$ and adjusting the pH by hydrochloric acid. No uranyl complex was obtained under the conditions mentioned above. These observations reveal that the acidic conditions and the strong oxidizing agent play important roles in the reaction. In addition, the syntheses are dependent remarkably on the reaction temperature, which is required at least 160 °C or higher. We also investigated the effect of metal medium and found that no transition metal-bearing crystalline hybrid materials were obtained when using other metal salts including $Zn(NO_3)_2$, $Cu(NO_3)_2$, and $Co(NO_3)_2$ replacing the $UO_2(NO_3)_2$ under similar conditions.

Scheme 1. In Situ DTPT Formation from DMPDP Mediated by Uranyl Cation under Hydrothermal Condition

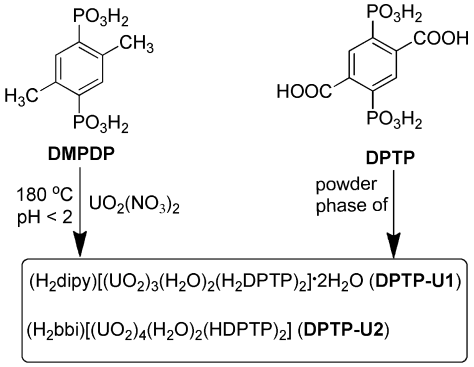

Structure of DPTP-U1. The asymmetric unit of **DPTP-U1** consists of two crystallographically unique uranium sites, one DPTP ligand, and half a dipy (Figure 1). U(1) atom is in a general position and seven coordinated by two "*yl*" oxygen atoms, five oxygen atoms from three phosphonate groups, one carboxylate moiety, and one water molecule in the equatorial plane, thus forming a common pentagonal bipyramidal geometry. U(2) is at the inversion center, and its coordination environment is defined by two symmetrical oxo atoms and four equatorial oxygen atoms from four phosphonate functional groups, thereby leading to a less common square bipyramidal sphere. The axial U=O bond lengths of the two uranium centers are in the range from 1.757(5) to ~1.767(5) Å, whereas, within the equatorial plane, the U–O bond lengths range from 2.264(5) to 2.506(6) Å. On the basis of these values, the calculated bond-valence sum for the uranium atoms indicates 6.21 for U(1) and 5.87 for U(2), which is consistent with the formal valence of U(VI).[36] The uranyl square and pentagonal bipyramids are bridged by the PO_3 groups, creating a uranyl phosphonate chain. Such chains are further linked by the phenyl spacers, therefore resulting in a layered structure (Figure 2a). The P(1) and P(2) phosphonate groups connect three and two uranyl centers, respectively, and the terminal O(7) is protonated (P(2)–O(7): 1.558(5) Å). One carboxylate

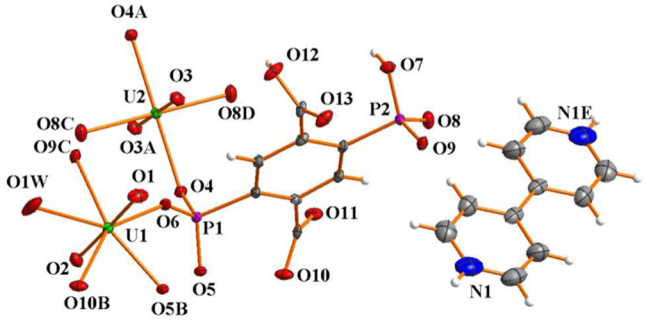

Figure 1. (a) ORTEP representation of the asymmetric unit in **DPTP-U1**. Thermal ellipsoids are drawn at the 50% probability level. Symmetry codes A: $1-x, -y, 1-z$; B: $1-x, -y, 2-z$; C: $x, -1+y, z$; D: $1-x, 1-y, 1-z$; E: $2-x, 2-y, 1-z$.

DOI: 10.1021/acs.inorgchem.5b01266
Inorg. Chem. 2015, 54, 8617–8624

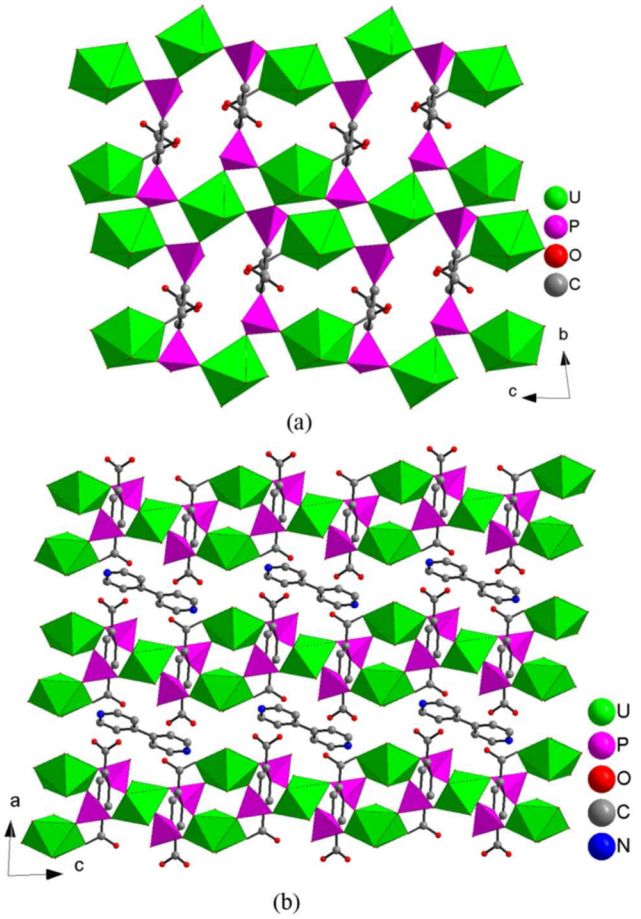

Figure 2. (a) The individual layer of **DPTP-U1**, in which the uranyl phosphonate chains are bridged by the phenyl rings. (b) The layers are stacked together along the *b* axis with the protonated dipy cations seated in the interlayer space. Hydrogen atoms are omitted for clarity.

moiety unidentately coordinates to the U(1) center, and the other carboxylate is idle, dangling into the interlayer space. This is consistent with the hard/soft acid/base theory[37] that the uranyl cations preferentially bind to the harder phosphonate group over the softer carboxylate group. As shown in Figure 2b, the uranyl phosphonate sheets stack along the *b* axis, separated by protonated dipy cations.

Structure of DPTP-U2. Different from **DPTP-U1**, **DPTP-U2** features a three-dimensional (3D) framework structure. As shown in Figure 3, there are two crystallographically distinct uranium atoms, one DPTP ligand, and half a bbi molecule in the asymmetric unit. Both of the uranium atoms are in the pentagonal bipyramidal surrounding defined by two axial oxygen atoms and five equatorial oxygen atoms. One carboxylate group and three phosphonate groups supply the O donors to complete the coordination sphere of U(1). For U(2), it also coordinates an additional water molecule. The inert U═O bonds of the two uranium atoms are at the distances from 1.754(12) to ~1.781(11) Å, and in the equatorial plane, the oxygen atoms are arranged fom 2.246(11) to ~2.597(11) Å away from the uranium centers. The valences of uranium atoms are 5.84 for U(1) and 5.89 for U(2) based on calculated bond-valence sum. Two U(1) centers condense to a uranyl dimer by sharing an edge. Such dimers together with mononuclear U(2) pentagonal bipyramids are chelated and bridged by PO_3 groups to form a uranyl

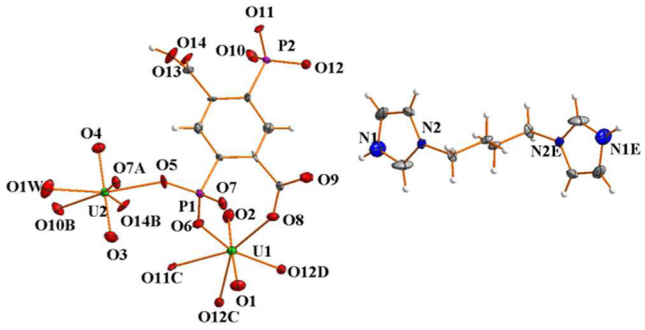

Figure 3. (a) ORTEP representation of the asymmetric unit in **DPTP-U2**. Thermal ellipsoids are drawn at the 50% probability level. Symmetry codes A: 2 − *x*, −*y*, −*z*; B: 2 − *x*, 1 − *y*, −*z*; C: 1 + *x*, *y*, *z*; D: 2 − *x*, 1 − *y*, 1 − *z*; E: 1 − *x*, −*y*, 1 − *z*.

phosphate sheet. The phenyl spacers serve as the columns to pillar the sheets and give rise to the 3D framework structure of **DPTP-U2** (Figure 4). This pillared structure contains one-dimensional (1D) channels along the *c* axis, which are filled by protonated bbi cations. Both of the carboxylate moieties adopt the unidentate coordination mode for binding the uranium

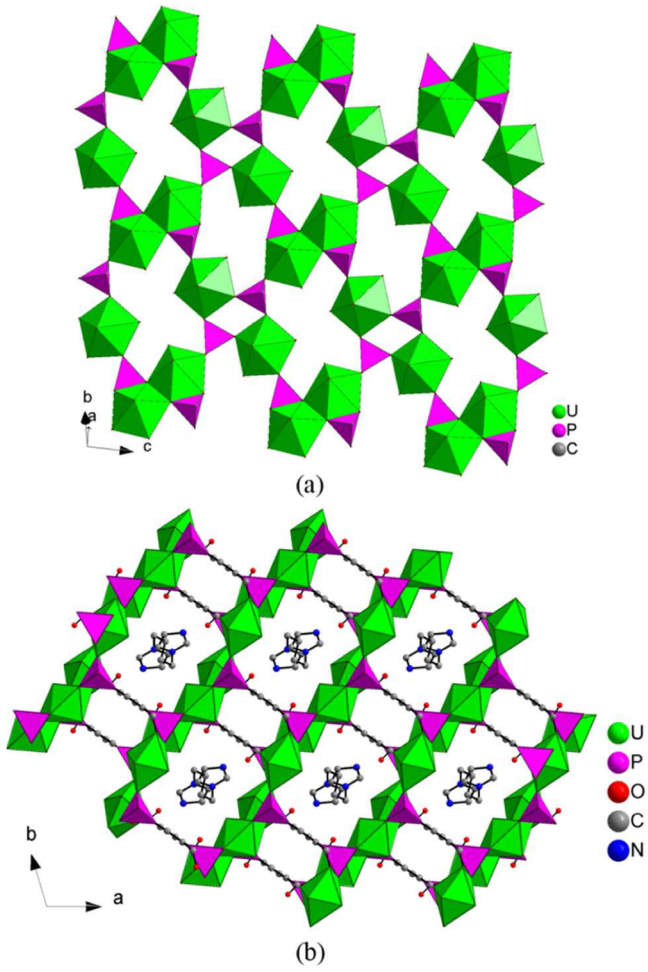

Figure 4. Uranyl pentagonal bipyramidal monomers and dimers are linked by PO_3 groups forming the sheets (a), which are pillared by the phenyl spacers to give the 3D framework of **DPTP-U2** with protonated bbi cations occupying the channels (b). Hydrogen atoms are omitted for clarity.

DOI: 10.1021/acs.inorgchem.5b01266
Inorg. Chem. 2015, 54, 8617−8624

centers, leaving the unbound O atoms terminal (C−O(9): 1.248(19) Å) and protonated (C−O(13): 1.291(19) Å), respectively.

Structure Discussion. It is known that the coordination sphere of uranyl center is usually completed by four to six coordinating atoms in the equatorial plane, leading to square, pentagonal, and hexagonal bipyramids. These three bipyramidal polyhedra not only can serve as primary building blocks but also can polymerize via corner-sharing and/or edge-sharing interactions forming various building units in constructing uranyl phosphonate structures.[22b] In **DPTP-U1**, monomers of UO_6 and UO_7 polyhedra act as the inorganic building units, while **DPTP-U2** contains monomers and edge-sharing dimers of UO_7 pentatgonal bipyramids. However, the carboxyphosphonate ligand adopts different coordination modes in connecting metal centers in the two uranyl compounds. The PO_3 groups in **DPTP-U1** ligate two uranium and three uranium centers, respectively, while for **DPTP-U2** both the phosphonate groups bind three uranium centers. Two carboxylate moieties of the ligand in **DPTP-U2** participate in connecting uranyl ions, whereas one carboxylate of the ligand in **DPTP-U1** is free. As a result, the ligands adopt $\mu_5(\eta_1{:}\eta_1{:}\eta_1{:}\eta_1{:}\eta_2)$ and $\mu_6(\eta_1{:}\eta_1{:}\eta_2{:}\eta_1{:}\eta_2{:}\eta_2)$ coordination modes, respectively, in **DPTP-U1** and **DPTP-U2**. So far, three aromatic carboxyphosphonate ligands, which are three isomers of carboxyphenylphosphonic acid, were used to isolate uranyl phosphonates, most of which are heterometallic uranyl compounds.[38] Only five homometallic uranyl compounds were reported.[39] The structures in this work enrich the series of homometallic uranyl carboxyphosphonates.

Theoretical Calculation Results. A detailed investigation on the electronic structures of the two new uranyl carboxyphosphonate compounds is presented here to analyze the mechanism of uranium complexation and to provide new insight into the nature of interactions between uranyl cation and the carboxyphosphonate ligand. As shown in Table 2, the bond lengths of the uranyl bonds (U═O) are predicted to be 1.80−1.82 Å in **DPTP-U1** and 1.79−1.80 Å in **DPTP-U2**, respectively. These values are in accord with the measured ones from our experiments. The equatorial coordination bonds (U−O) are determined to be 2.26−2.59 Å for **DPTP-U1** and 2.27−2.52 Å for **DPTP-U2**, which are also in good agreement with the experiments. The average relative error between the calculated and experimental bond distances is ∼1.7%, and the maximum error is below 3.5%. It should be mentioned that the predicted sequence of bond lengths from the longest to the shortest also coincides very well with that from the experiments. Therefore, the geometries of the compounds are well-reproduced in our theoretical study. The bond population is useful for evaluating the bonding character in a material and a high value of the population indicates a strong covalent bond.[40] The corresponding data are also listed in Table 2.

Table 2. Selected Calculated Bond Distances (Å) for Title Compounds

DPTP-U1			DPTP-U2		
bond	population	length (Å)	bond	population	length (Å)
O1−U1	0.63	1.801	O1−U1	0.66	1.802
O2−U1	0.67	1.821	O2−U1	0.65	1.805
O1W−U1	0.02	2.591	P1−O6−U1	0.26	2.279
P1−O5B−U1	0.27	2.321	C−O8−U1	0.22	2.320
P2−O9C−U1	0.25	2.360	P2−O12D−U1	0.16	2.410
P1−O6−U1	0.27	2.267	P2−O11C−U1	0.08	2.505
C−O10B−U1	0.19	2.511	P2−O12C−U1	0.07	2.523
O3A-U2	0.67	1.806	O3−U2	0.67	1.796
O3−U2	0.67	1.806	O4−U2	0.69	1.808
P2−O8D−U2	0.23	2.313	O1W−U2	0.08	2.515
P2−O8C−U2	0.23	2.313	P1−O7A−U2	0.24	2.385
P1−O4A−U2	0.23	2.342	P2−O10B−U2	0.18	2.361
P1−O4−U2	0.23	2.342	P1−O5−U2	0.27	2.305
			C−O14B−U2	0.19	2.468

In **DPTP-U1**, the U(1) atom is predicted to be located in the center of pentagonal bipyramid and seven-coordinated, and the U(2) atom is determined in the inversion center of a tetragonal bipyramid and six-coordinated. The geometries are consistent well with the experiments. It is apparent that the O(1W)−U(1) bond formed by the water molecule and the uranium center is the weakest among all uranyl equatorial coordination bonds from Table 2, reflected by its longest bond length (2.59 Å) and lowest bond population (0.02) among all O−U(1)/O−U(2) bonds. These findings may imply that coordinate water acts as the weakest ligand relative to other groups and that the direct contribution of water molecule in the stabilization of uranium complexes is negligible. Nevertheless, this also indicates the stability of the new compound **DPTP-U1** does not rely on the aqueous environment, which means the uranyl ions are unlikely to be dissolved into a liquid phase in a wet environment and thus is an advantage for developing nuclear separation. Within all the equatorial atoms from phosphonate groups, one can find that the bond populations of O(P1)−U(1)are higher than those of O(P1)−U(2), meaning that the coordination of phosphonate P(1) to U(1) is stronger than (P1) to U(2) and that the O(P1)−U(1) bonds are also determined to be stronger than the O(P2)−U(1) based on the corresponding bond lengths. In addition, it is interesting to point out that the O(10)−U(1)bond, which results from the interaction of uranium and the carboxylate moiety, is the longest among all O−U bonds except for O(1W)−U(1,2) according to Table 2. This is an indication that the interaction between carboxyl and center uranyl is weaker than that involved by phosphonate, which may be attributed to the more covalent feature of a C═O bond than a P═O bond.

As to the compound **DPTP-U2**, the structure also consists of two types of uranyl centers U(1) and U(2), both of which are predicted to be seven-coordinated, differing from **DPTP-U1**. These findings are consistent with the experiments, as well. The two U(1) centers condense to a uranyl dimer by a bridging oxygen atom, which is absent for the U(2) centers, which well resembles the laboratory observations. At the equatorial positions, both uranium atoms are coordinated with oxygen atoms from carboxylate and phosphonate. Meanwhile the U(2) atom also coordinates an additional water molecule. For the coordinate bonds formed by uranium and carboxylate group, the O(8)−U(1) bond is determined to be stronger than O(14)−U(2) by comparing their bond lengths and bond populations. It can also be found by population analysis that C−O(8)−U(1) is stronger than that of P(2)−O−U(1) and that the magnitude of bond population for C−O(8)−U(1) is

DOI: 10.1021/acs.inorgchem.5b01266
Inorg. Chem. 2015, 54, 8617−8624

only slightly lower than that of P(1)−O(6)−U(1), indicating contribution of the carboxyl group is significant for the stabilization for **DPTP-U2**. Furthermore, the difference of bond populations between C−O(14)−U(2) and P(1)−O(5)−U(2) is larger than that between C−O(8)−U(1) and P(1)−O(6)−U(1), showing that the significance of the equatorial bonding effect originated from carboxyl groups and uranyl may depend on the chemical environment of the uranium atom. In **DPTP-U2**, it can be readily seen that the O−U(1) bond distances from P(1) phosphonates are shorter than that of P(2) phosphonates and that the corresponding bond populations from P(1) are also larger than P(2). This obvious difference in bonding effect may be attributed to the fact that P(1) forms coordination bonds with three unbridged uranium atoms [one U(1) and two U(2)], while two of the three U atoms that P(2) is ligated to are bridged [two U(1)]. The coordination to bridged atoms may obstruct the formation of optimal P(2)−O−U(1) bonds due to the additional geometrical constraints. As to O−U(2) bonds from P(1) and P(2) phosphonates, the coordination of the former to the uranium atom is also determined to be stronger. Similar to the **DPTP-U1**, the bond distance of uranium and the crystalliferous water molecules in **DPTP-U2** is as long as 2.51 Å, and thus this bond is much weaker than the other equatorial coordination bonds. Hence the weak coordination effect of crystalliferous water is a common feature that favors the stability in an aqueous environment for both **DPTP-U1** and **DPTP-U2** when they are used in the spent nuclear fuel cycle.

According to the above analysis, the general feature for **DPTP-U1** and **DPTP-U2** is that the phosphonate group is stronger in coordination strength than carboxyl groups and water molecules. However, weak water coordination bonds indicate little influence of the wet environment on the structures; when the bridge bonds in U(1) of **DPTP-U2** elongate some P−O−U bond distances, the coordination of U(1) to carboxyl group may become important and compensate the weakening effect. Consequently, the concerted effect of hybrid coordination leads to stable crystalline structures, although the P−O−U coordination bonds play the dominant role for both compounds synthesized in this work. Since the complexes with P═O bond coordinated to U(VI) have been shown to play an important role in recycling of used nuclear fuel,[41] the two novel uranium carboxyphosphonates **DPTP-U1** and **DPTP-U2** may also be an option for the application of crystallization-based actinide separations in nuclear fuel cycle.

The total and partial density of states (DOS) for **DPTP-U1** and **DPTP-U2** are shown in Figure 5, which provides a deeper insight into the nature of the chemical bonds in the equatorial plane. In Figure 5a, the DOS for U(1) and U(2) in **DPTP-U1** show similar characteristics. From −2.0 eV to the Fermi level, the 2p orbital of O(1w) overlaps scarcely with the f-orbital of U(1). By contrast, the valence band maximum (VBM) peaks of other equatorial oxygen atoms from phosphonates (O(6), O(4)) and carboxylate (O10) upshift to the Fermi level apparently, allowing more overlapping with the f-electron of U atoms. This suggests that the equatorial oxygen atoms from carboxyl and phsophonate groups provide relatively strong coordination bond with uranyl. The result is consistent with the sequence of the corresponding bond populations. Moreover, the overlapping of the f-orbital of uranium with the p-orbital of O(6) and O(4) near −2.0 eV is larger than that for O(10). This agrees well with the larger bond populations of O(6) and O(4)

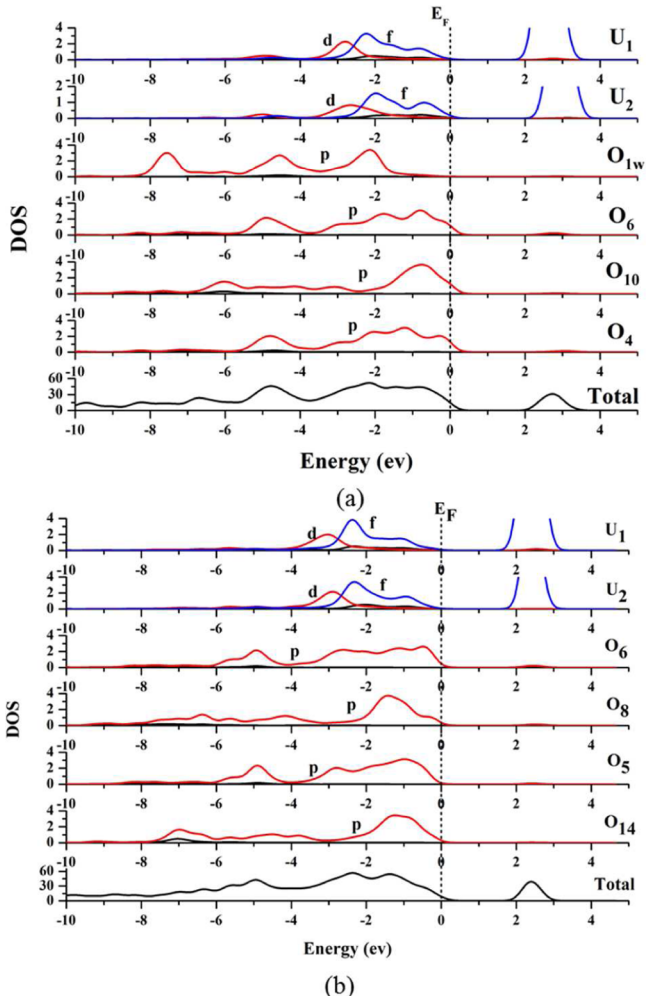

Figure 5. Total and selected partial densities of states of **DPTP-U1** (a) and **DPTP-U2** (b).

listed in Table 2. These results provide evidence that explains the phosphonate group has a stronger interaction with uranium atom than carboxyl in **DPTP-U1**. Finally, the relative strength of O(6)−U(1) and O(4)−U(2) can be determined by the greater overlapping at $E = -0.8$ eV for O(6) than O(4). This is a reflection that electrons from O(6) contribute more to the interaction between uranium and oxygen than other equatorial coordinates.

In Figure 5b, one can find that the peaks of O(6)-2p and O(5)-2p originating from P(1) are broader than that of O(8) and O(14) from carboxyl groups. The similarities in the forms of partial DOS between O(5) and O(6) and between O(8) and O(14) indicate that the bonding feature is strongly correlated with the functional group that the oxygen atoms belongs to. It is interesting to note that the broadness of the partial DOS near the Fermi level for the oxygen atoms from carboxyl group is similar to that in **DPTP-U1**. The current result suggests that the overlapping of the 2p orbitals of oxygen atoms O(5) and O(6) from phosphonate with the f-orbitals of U(1,2) is greater with the orbital energy ranging from −3 to −2 eV than O(8) and O(14). These results demonstrate that the phosphonate group significantly contributes to the stability of **DPTP-U2**, which is consistent well with the findings from the bond populations of **DPTP-U2** presented in Table 2.

DOI: 10.1021/acs.inorgchem.5b01266
Inorg. Chem. 2015, 54, 8617−8624

IR, UV−vis−NIR, and Luminescent Spectroscopy. The IR spectra of **DPTP-U1** and **DPTP-U2** as well as DMPDP and DPTP ligands were recorded (Figure S4). The spectrum of DPTP exhibits characteristic absorption peaks of carboxylic acid at 1280 (ν_{C-OH}) and 1631 and 1708 cm^{-1} ($\nu_{C=O}$), which are not visible in the spectrum of DMPDP. The newly observed peaks in the IR spectrum of DPTP clearly confirm the in situ formation of carboxylic acid group in the reaction. In comparison, the spectra of uranyl compounds **DPTP-U1** and **DPTP-U2** show adsorption bands in the range of 1411−1670 cm^{-1}, which are associated with the stretching vibrations of carboxylate group. In addition, the broad bands from 3300 to 3630 cm^{-1} in the IR spectra of **DPTP-U1** and **DPTP-U2** are attributed to the lattice and coordinated water molecules. The symmetric and asymmetric stretching vibration of the U═O bond of the uranyl cation are observed at ∼824 and 923 cm^{-1}, respectively, in the spectra of **DPTP-U1** and **DPTP-U2**.

As shown in Figure S5, the solid-state UV−vis absorption spectra of **DPTP-U1** and **DPTP-U2** both display the vibronically coupled charge transfer band of hexavalent uranium species in the region of 380−510 nm. The adsorption band of **DPTP-U1** splits into five peaks positioned at 424, 451, 467, 482, and 497 nm; for **DPTP-U2**, splitting does not occur, and the band is centered at 420 nm. Both of the adsorption spectra of the two compounds exhibit the typical vibronic progression from the uranyl ion and are similar to those previously reported uranyl phosphonate compounds.[41,42] Besides, the broad peaks centered at ∼350 nm for both compounds are probably due to the ligand-to-metal charge transfer.[43]

The emission of green light centered near 520 nm by U(VI)-bearing compounds has been documented for decades. This charge-transfer based emission is always related to the symmetric and antisymmetric vibrational modes of the UO_2^{2+} cation, and there are usually five to six typical peaks in the spectrum. Here the photoluminescent properties of **DPTP-U1** and **DPTP-U2** were also studied, and the spectra are illustrated in Figure 6. Multiple emission peaks are clearly resolved for **DPTP-U1** (502, 524, 547, and 571 nm) and **DPTP-U2** (505, 527, 550, 576, and 605 nm), which correspond to the electronic and vibronic transitions $S_{11}-S_{00}$ and $S_{10}-S_{0v}$, where v = 0−4. This charge-transfer based emission is typical for uranyl-bearing materials. Compared to the benchmark compound $UO_2(NO_3)_2{\cdot}6H_2O$[44] the spectra are red-shifted by 15 and 18 nm for **DPTP-U1** and **DPTP-U2**, respectively. The luminescent spectra from the two compounds are similar to those reported for other homometallic uranyl carboxyphosphonate compounds.[39] The slight difference in spectra of **DPTP-U1** and **DPTP-U2** may originate from the different coordination environments (UO_6 and UO_7), polymerization of primary building units, and the influence of the carboxyphosphonate ligand and organic templates.

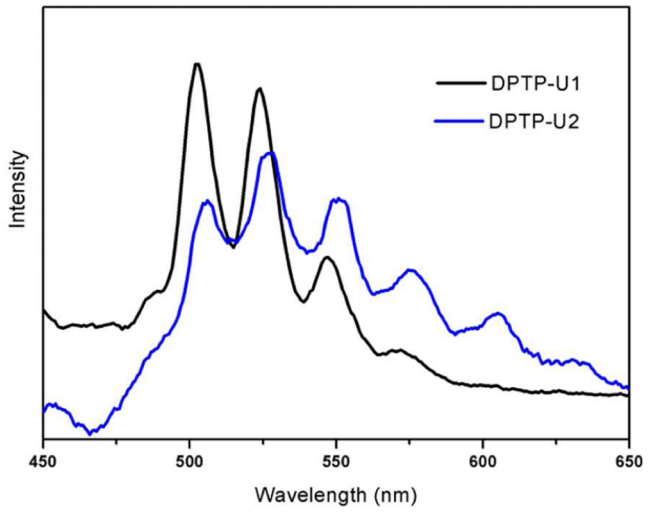

Figure 6. Emission spectra of **DPTP-U1** and **DPTP-U2**.

CONCLUSION

In this present contribution, we have synthesized two novel uranyl carboxyphosphonates from the in situ ligand reaction under hydrothermal conditions. Both compounds adopt the phosphonate and in situ generated carboxylate groups for binding the uranium centers. In **DPTP-U1**, uranyl pentagonal and square bipyramidal spheres are ligated by DPTP ligands, forming a layered structure with protonated dipy cations occupying the interlayer space, while in **DPTP-U2**, pentagonal bipyramidal uranyl monomers and dimers are linked by the carboxyphosphonate ligands to produce a 3D framework structure, which exhibits 1D channels filled by protonated bbi cations. The analyses on the electronic structures indicate that the two novel uranium carboxyphosphonates would be promising materials for the crystallization-based actinide separations. Our investigations demonstrate that in situ ligand reaction is a powerful tactic to construct uranium organic coordination polymers with novel ligands. Further research into new in situ ligand reactions in syntheses of uranium compounds is ongoing in our laboratory.

ASSOCIATED CONTENT

Supporting Information

The Supporting Information is available free of charge on the ACS Publications website at DOI: 10.1021/acs.inorgchem.5b01266.

Selected bond lengths and angles, simulated and experimental PXRD patterns, IR, and UV−vis−NIR spectroscopy. (PDF)

X-ray crystallographic information pertaining to three structures. (CIF)

AUTHOR INFORMATION

Corresponding Authors

*E-mail: wtyang@ciac.ac.cn. (W.Y.)
*E-mail: szm@ciac.ac.cn. (Z.-M.S.)
*E-mail: dushiyu@nimte.ac.cn. (S.D.)

Author Contributions

‖These authors contributed equally.

Notes

The authors declare no competing financial interest.

ACKNOWLEDGMENTS

We are thankful for the support of this work by ITaP at Purdue University, West Lafayette, IN for computing resources, National Nature Science Foundation of China (Nos. 21171162, 21301168, and U1407101), Jilin Province Youth Foundation (20130522132JH and 20130522123JH), the key technology of nuclear energy, 2014, CAS Interdisciplinary Innovation Team, and SRF for ROCS (State Education

DOI: 10.1021/acs.inorgchem.5b01266
Inorg. Chem. 2015, 54, 8617−8624

Ministry). We thank Prof. S.-F. Tang and Prof. S. Wang for their valuable discussions.

REFERENCES

(1) Zhao, H.; Qu, Z. R.; Ye, H. Y.; Xiong, R. G. *Chem. Soc. Rev.* **2008**, *37*, 84−100.
(2) Chen, X. M.; Tong, M. L. *Acc. Chem. Res.* **2007**, *40*, 162−170.
(3) Zhang, X. M. *Coord. Chem. Rev.* **2005**, *249*, 1201−1219.
(4) Zhang, X. M.; Tong, M. L.; Chen, X. M. *Angew. Chem., Int. Ed.* **2002**, *41*, 1029−1031.
(5) Wang, X.; Yang, J.; Zhang, L.; Liu, F.; Dai, F.; Sun, D. *Inorg. Chem.* **2014**, *53*, 11206−11212.
(6) Cheng, J. K.; Yao, Y. G.; Zhang, J.; Li, Z. J.; Cai, Z. W.; Zhang, X. Y.; Chen, Z. N.; Chen, Y. B.; Kang, Y.; Qin, Y. Y.; Wen, Y. H. *J. Am. Chem. Soc.* **2004**, *126*, 7796−7797.
(7) Lee, J. Y.; Hong, S. J.; Kim, C.; Kim, Y. *Dalton Trans.* **2005**, 3716−3718.
(8) Xiong, R. G.; Xue, X.; Zhao, H.; You, X. Z.; Abrahams, B. F.; Xue, Z. L. *Angew. Chem., Int. Ed.* **2002**, *41*, 3800−3803.
(9) Hu, X. X.; Xu, J. Q.; Cheng, P.; Chen, X. Y.; Cui, X. B.; Song, J. F.; Yang, G. D.; Wang, T. G. *Inorg. Chem.* **2004**, *43*, 2261−2266.
(10) Chen, Q.; Jiang, F.; Chen, L.; Yang, M.; Hong, M. *Chem. - Eur. J.* **2012**, *18*, 9117−9124.
(11) Han, Z.; Zhao, Y.; Peng, J.; Gomez-Garcia, C. J. *Inorg. Chem.* **2007**, *46*, 5453−5455.
(12) Andrews, M. B.; Cahill, C. L. *Angew. Chem., Int. Ed.* **2012**, *51*, 6631−6634.
(13) Knope, K. E.; Cahill, C. L. *CrystEngComm* **2011**, *13*, 153−157.
(14) Knope, K. E.; Cahill, C. L. *Inorg. Chem.* **2007**, *46*, 6607−6612.
(15) Andrews, M. B.; Cahill, C. L. *CrystEngComm* **2011**, *13*, 7068−7078.
(16) Yang, W.; Wang, H.; Du, Z. Y.; Tian, W. G.; Sun, Z. M. *CrystEngComm* **2014**, *16*, 8073−8080.
(17) (a) Iremonger, S. S.; Liang, J.; Vaidhyanathan, R.; Martens, I.; Shimizu, G. K. H.; Daff, T. D.; Aghaji, M. Z.; Yeganegi, S.; Woo, T. K. *J. Am. Chem. Soc.* **2011**, *133*, 20048−20051. (b) Iremonger, S. S.; Liang, J.; Vaidhyanathan, R.; Shimizu, G. K. H. *Chem. Commun.* **2011**, *47*, 4430−4432. (c) Breen, J. M.; Schmitt, W. *Angew. Chem., Int. Ed.* **2008**, *47*, 6904−6908. (d) Poojary, D. M.; Zhang, B.; Bellinghausen, P.; Clearfield, A. *Inorg. Chem.* **1996**, *35*, 4942−4949.
(18) (a) Bialek, M. J.; Janczak, J.; Zoń, J. *CrystEngComm* **2013**, *15*, 390−399. (b) Amghouz, Z.; García-Granda, S.; García, J. R.; Clearfield, A.; Valiente, R. *Cryst. Growth Des.* **2011**, *11*, 5289−5297.
(19) (a) Adelani, P. O.; Albrecht-Schmitt, T. E. *J. Solid State Chem.* **2012**, *192*, 377−384. (b) Adelani, P. O.; Albrecht-Schmitt, T. E. *Angew. Chem., Int. Ed.* **2010**, *49*, 8909−8911. (c) Adelani, P. O.; Albrecht-Schmitt, T. E. *Inorg. Chem.* **2009**, *48*, 2732−2734. (d) Adelani, P. O.; Albrecht-Schmitt, T. E. *J. Solid State Chem.* **2011**, *184*, 2368−2373. (e) Adelani, P. O.; Albrecht-Schmitt, T. E. *Cryst. Growth Des.* **2011**, *11*, 4227−4237.
(20) Tang, S. F.; Li, L. J.; Lv, X. X.; Wang, C.; Zhao, X. B. *CrystEngComm* **2014**, *16*, 7043−7052.
(21) (a) Fan, L. L.; Li, C. J.; Meng, Z. S.; Tong, M. L. *Eur. J. Inorg. Chem.* **2008**, *2008*, 3905−3909. (b) Li, C. J.; Lin, Z.; Yun, L.; Xie, Y. L.; Leng, J. D.; Ou, Y. C.; Tong, M. L. *CrystEngComm* **2010**, *12*, 425−433. (c) Ma, D.; Wang, W.; Li, Y.; Li, J.; Daiguebonne, C.; Calvez, G.; Guillou, O. *CrystEngComm* **2010**, *12*, 4372−4377.
(22) (a) Knope, K. E.; Cahill, C. L. Uranyl Phosphonates: A Structural Survey. In *Metal Phosphonate Chemistry: From Synthesis to Applications;* Clearfield, A., Demadis, K., Eds.; The Royal Society of Chemistry: London, U.K., 2012, 586−606. (b) Yang, W.; Parker, T. G.; Sun, Z. M. *Coord. Chem. Rev.* **2015**, *303*, 86−109. (c) Yang, W.; Yi, F. Y.; Tian, T.; Tian, W. G.; Sun, Z. M. *Cryst. Growth Des.* **2014**, *14*, 1366−1374. (d) Yang, W.; Tian, T.; Wu, H. Y.; Pan, Q. J.; Dang, S.; Sun, Z. M. *Inorg. Chem.* **2013**, *52*, 2736−2743.
(23) (a) Wang, K. X.; Chen, J. S. *Acc. Chem. Res.* **2011**, *44*, 531−540. (b) Yu, Z. T.; Liao, Z. L.; Jiang, Y. S.; Li, G. H.; Chen, J. S. *Chem. - Eur. J.* **2005**, *11*, 2642−2650. (c) Liao, Z. L.; Li, G. D.; Bi, M. H.; Chen, J. S. *Inorg. Chem.* **2008**, *47*, 4844−4852.
(24) (a) Loiseau, T.; Mihalcea, I.; Henry, N.; Volkringer, C. *Coord. Chem. Rev.* **2014**, *266−267*, 69−109. (b) Olchowka, J.; Falaise, C.; Volkringer, C.; Henry, N.; Loiseau, T. *Chem. - Eur. J.* **2013**, *19*, 2012−2022. (c) Volkringer, C.; Henry, N.; Grandjean, S.; Loiseau, T. *J. Am. Chem. Soc.* **2012**, *134*, 1275−1283.
(25) (a) Qiu, J.; Burns, P. C. *Chem. Rev.* **2013**, *113*, 1097−1120. (b) Weng, Z. H.; Zhang, Z. H.; Olds, T.; Sterniczuk, M.; Burns, P. C. *Inorg. Chem.* **2014**, *53*, 7993−7998. (c) Adelani, P. O.; Cook, N. D.; Burns, P. C. *Cryst. Growth Des.* **2014**, *14*, 5692−5699.
(26) (a) Thuery, P.; Harrowfield, J. *Cryst. Growth Des.* **2014**, *14*, 1314−1323. (b) Thuery, P. *Inorg. Chem.* **2013**, *52*, 435−447.
(27) (a) Tiferet, E.; Gil, A.; Bo, C.; Shvareva, T. Y.; Nyman, M.; Navrotsky, A. *Chem. - Eur. J.* **2014**, *20*, 3646−3651. (b) Liao, Z. L.; Deb, T.; Nyman, M. *Inorg. Chem.* **2014**, *53*, 10506−10513. (c) Arnold, P. L.; Stevens, C. J.; Farnaby, J. H.; Gardiner, M. G.; Nichol, G. S.; Love, J. B. *J. Am. Chem. Soc.* **2014**, *136*, 10218−10221. (d) Jones, G. M.; Arnold, P. L.; Love, J. B. *Chem. - Eur. J.* **2013**, *19*, 10287−10294.
(28) Bengtsson, E. B. *Acta Chem. Scand.* **1953**, *7*, 774−780.
(29) Sheldrick, G. M. *SHELXTL 6.10;* Bruker-AXS X-Ray Instrumentation Inc: Madison, WI, 2000.
(30) Hohenberg, P.; Kohn, W. *Phys. Rev.* **1964**, *136*, B864−B871.
(31) (a) Clark, S. J.; Segall, M. D.; Pickard, C. J.; Hasnip, P. J.; Probert, M. J.; Refson, K.; Payne, M. C. *Z. Kristallogr.* **2005**, *220*, 567−570. (b) Segall, M. D.; Lindan, P. J. D.; Probert, M. J.; Pickard, C. J.; Hasnip, P. J.; Clark, S. J.; Payne, M. C. *J. Phys.: Condens. Matter* **2002**, *14*, 2717−2744.
(32) (a) Perdew, J. P.; Ernzerhof, M.; Burke, K. *Phys. Rev. Lett.* **1996**, *77*, 3865−3868. (b) Perdew, J. P.; Chevary, J. A.; Vosko, S. H.; Jackson, K. A.; Pederson, M. R.; Singh, D. J.; Fiolhais, C. *Phys. Rev. B: Condens. Matter Mater. Phys.* **1992**, *46*, 6671−6687.
(33) (a) Payne, M. C.; Teter, M. P.; Allan, D. C.; Arias, T. A.; Joannopoulos, J. D. *Rev. Mod. Phys.* **1992**, *64*, 1045−1097. (b) Monkhorst, H. J.; Pack, J. D. *Phys. Rev. B* **1976**, *13*, 5188−5192.
(34) (a) Kohn, W.; Sham, L. J. *Phys. Rev.* **1965**, *140*, A1133−A1138. (b) Vanderbilt, D. *Phys. Rev. B: Condens. Matter Mater. Phys.* **1990**, *41*, 7892−7895.
(35) Alsobrook, A. N.; Hauser, B. G.; Hupp, J. T.; Alekseev, E. V.; Depmeier, W.; Albrecht-Schmitt, T. E. *Chem. Commun.* **2010**, *46*, 9167−9169.
(36) (a) Burns, P. C.; Ewing, R. C.; Hawthorne, F. C.; Miller, M.; Finck, R. J. *MRS Online Proc. Libr.* **1997**, *35*, 1551−1570. (b) Brese, N. E.; O'Keeffe, M. *Acta Crystallogr., Sect. B: Struct. Sci.* **1991**, *B47*, 192−197.
(37) Pearson, R. G. *J. Chem. Educ.* **1968**, *45*, 581−586.
(38) (a) Adelani, P. O.; Albrecht-Schmitt, T. E. *Cryst. Growth Des.* **2011**, *11*, 4676−4683. (b) Adelani, P. O.; Oliver, A. G.; Albrecht-Schmitt, T. E. *Inorg. Chem.* **2012**, *51*, 4885−4887.
(39) (a) Adelani, P. O.; Albrecht-Schmitt, T. E. *Inorg. Chem.* **2010**, *49*, 5701−5705. (b) Adelani, P. O.; Oliver, A. G.; Albrecht-Schmitt, T. E. *Cryst. Growth Des.* **2011**, *11*, 3072−3080.
(40) Mulliken, R. S. *J. Chem. Phys.* **1955**, *23*, 1833−1840.
(41) Zheng, T.; Wu, Q. Y.; Gao, Y.; Gui, D.; Qiu, S.; Chen, L.; Sheng, D.; Diwu, J.; Shi, W. Q.; Chai, Z.; Albrecht-Schmitt, T. E.; Wang, S. *Inorg. Chem.* **2015**, *54*, 3864−3874.
(42) Grohol, D.; Clearfield, A. *J. Am. Chem. Soc.* **1997**, *119*, 4662−4668.
(43) Parker, T. G.; Cross, J. N.; Polinski, M. J.; Lin, J.; Albrecht-Schmitt, T. E. *Cryst. Growth Des.* **2014**, *14*, 228−235.
(44) Adelani, P. O.; Oliver, A. G.; Albrecht-Schmitt, T. E. *Cryst. Growth Des.* **2011**, *11*, 1966−1973.

DOI: 10.1021/acs.inorgchem.5b01266
Inorg. Chem. 2015, 54, 8617−8624